Assessing the W2-AM for use in profiling x-ray optics

William P. Kuhn

William P. Kuhn, "Assessing the W2-AM for use in profiling x-ray optics," Proc. SPIE 10747, Optical System Alignment, Tolerancing, and Verification XII, 107470C (19 September 2018); doi: 10.1117/12.2323280

SPIE.

Event: SPIE Optical Engineering + Applications, 2018, San Diego, California, United States

Assessing the W2-AM for use in profiling x-ray optics

William P. Kuhn
Opt-E, 3450 S Broadmont Dr Ste 112, Tucson, AZ, USA 85713-5245

ABSTRACT

There is a long history of non-contact profilometry of mirrors performed using an autocollimator. An autocollimator is scanned over a mirror resulting in a set of local slope measurements that are then integrated to produce a measurement of the mirror profile. Such profilometers are often associated with the testing of x-ray optics. In this application a small beam is usually created by placing an aperture near the mirror under test. The W2-AM uses a reticle with a circular target. The noise, sensitivity and error characteristics of the W2-AM instrument is assessed relative to the needs of profilometry of x-ray optics.

Keywords: autostigmatic, autocollimator, optical alignment, profilometry, x-ray optics, optical metrology

1. INTRODUCTION

1.1 History

X-ray optics are typically designed for use at grazing incidence resulting in optical elements having very large length-to-width ratios, a very long radii-of-curvature in one direction and very short in the other direction. Due to the very short use wavelength figure and slope error requirements are quite demanding. An early metrology device is the Long Trace Profiler (LTP)[1], which utilizes a pencil-beam interferometer. A more recent device is the Nano-Optic-Measuring Machine (NOM)[2], an instrument that is approaching sub-50 nanoradian (nrad) measurements utilizing an Elcomat 3000 autocollimator. Another step further from the NOM is the Nano-surface profiling (NSP)[3] instrument, that also uses the Elcomat autocollimator.

The Elcomat autocollimator has a 50 mm aperture, 300 mm focal length and weighs about 3.8 kg. The autocollimator must be calibrated to address cycling errors, which has been done at the Physikalisch-Technische Bundesanstalt Braunschweig und Berlin (PTB) using their primary angle reference standard, the Heidenhain WMT220 angle comparator. The WMT220 that has an uncertainty of 0.001 arcsec (4.85 nrad); however, the calibration is performed at a fixed distance. An essential difference between the NOM and NSP is that the latter moves the entire autocollimator rather than a prism so that the distance to the sample is kept constant.

1.2 A possible alternative

The Elcomat 3000 residual error for the NOM[2] is 269 nrad rms. However, by calibrating and employing optimized operating methods, 50 nrad rms accuracy on plane mirrors is possible, but other mirror shapes are more difficult. the NSP approach is reaching the 50 nrad rms goal with a path towards further improvements in performance and generalization to other shapes.

Previous results with the W2-AM[4,5] showed centroid stability of about 0.003 pixels rms, or 100 nrad rms. Stability of the centroid measurement is obviously not the same as accuracy; however, stability sets a limit on potential accuracy. These previous results with the W2-AM suggest that it might be possible to reach the necessary measurement stability and implying at least the possibility of reaching the desired accuracy.

The 100 nrad rms stability measurement for the W2-AM was obtained using a 0.2 mm diameter circular obscuration as the alignment feature on a 7.1 mm x 5.3 mm detector having 3.45 μm square pixels. The obscuration size has been increased to 1 mm diameter and could be increased further. However, improving the centroid measurement of the point-spread function (PSF) produced from a pinhole is desirable to avoid any possible adverse effect from looking at an extended object on what will ultimately be very non-rotationally symmetric surfaces.

Optical System Alignment, Tolerancing, and Verification XII, edited by José Sasian
Richard N. Youngworth, Proc. of SPIE Vol. 10747, 107470C · © 2018 SPIE
CCC code: 0277-786X/18/$18 · doi: 10.1117/12.2323280

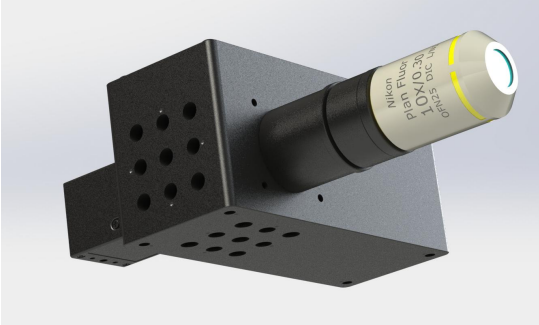

Figure 1. W2 alignment module with 100 mm focal length collimating lens and Nikon 10x objective installed. Removing the objective exposes a 12 mm diameter collimated beam with the standard 100 mm focal length collimating lens.

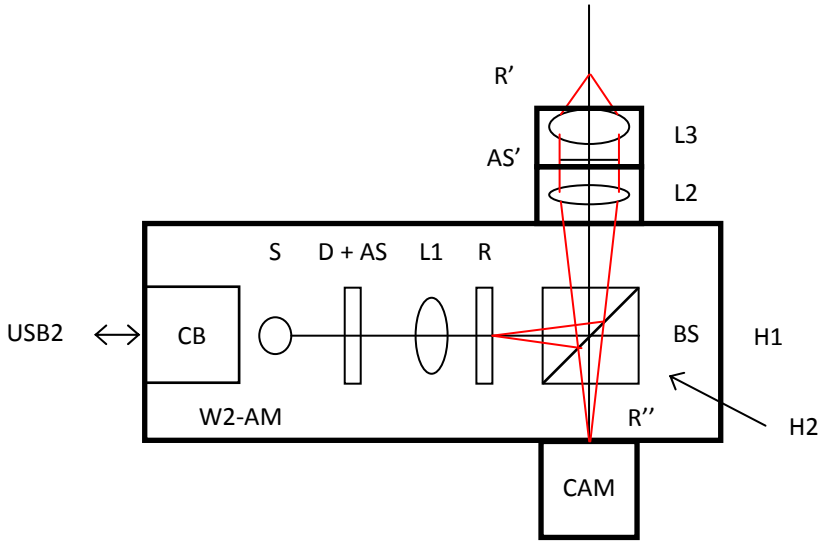

Figure 2. W2 alignment module schematic layout.

The schematic layout (Figure 2) illustrates the essential features of the instrument. The components are as follows:

1. USB2 – computer connection,
2. CB – circuit board,
3. S – source LED,
4. D + AS – diffuser and aperture stop,
5. L1 – condenser lens,
6. R – reticle (field stop),
7. BS – 1" beam splitter cube,
8. L2 – collimating lens assembly,
9. AS' – image of aperture stop,
10. L3 – optional focusing lens (e.g. microscope objective),
11. R' – finite conjugate image of R with L3 installed, or at infinity without L3,
12. R'' – image of reticle after projection and return, with or without L3,
13. CAM – C-mount camera,
14. H1 – hole pattern on enclosure side,
15. H2 – hole pattern on enclosure bottom, and
16. W2-AM – alignment module assembly and enclosure.

The core of the W2 optics is a Köhler illuminator and a cube beam splitter. The cube adds spherical aberration to a diverging or converging beam; however, at F/10 or slower, the aberration is negligible. The cube also adds longitudinal color, but the sources used are typically narrow band. Unlike a plate beam splitter, the cube does not add coma or astigmatism to a diverging or converging beam. The W2-AM weighs approximately 0.5 kg.

1.3 Reticle and images

The following image (Figure 3) is a captured image of the reticle pattern in a confocal or autostigmatic imaging configuration. The specific setup is focused at the center-of-curvature of a silicon nitride tooling ball, but it has the same appearance as if the instrument work aligned in autocollimator mode to a plane mirror, which is a lack of fine detail in the illuminated area since there is no surface located in this region. The pair of images in Figure 4 are magnified versions of the image in Figure 3 including the point spread function (PSF).

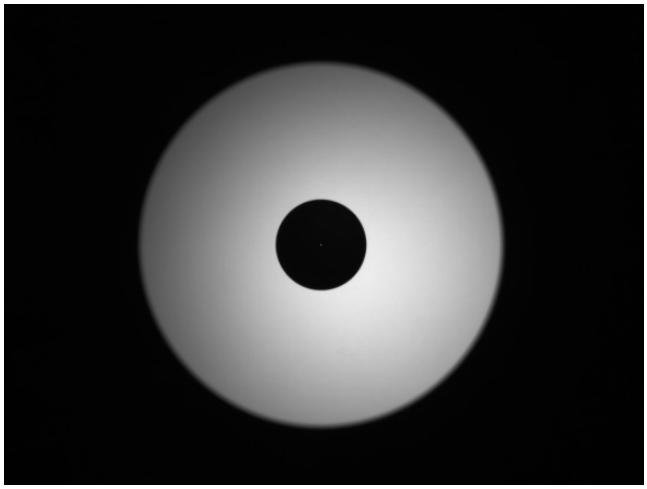

Figure 3. W2 full-frame image in autostigmatic imaging mode. An autocollimator image from a plane mirror would look the same.

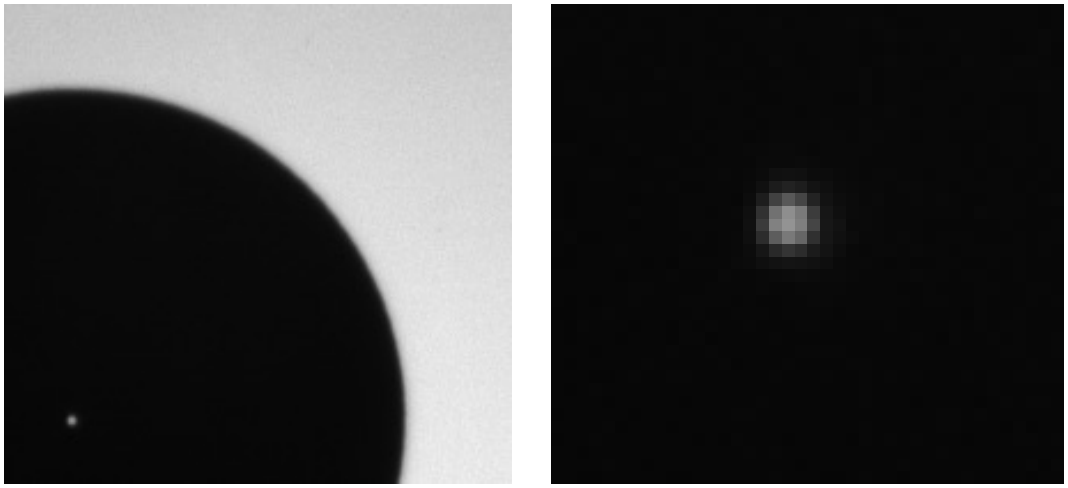

Figure 4. Zoomed in images showing the PSF detail.

1.4 Centroid calculation

The centroids of the obscuration and PSF are calculated from the image data. The process begins by finding the binary region of pixels below a threshold corresponding to the obscuration. Any missing pixels in this binary region, including

the pixels corresponding to the PSF, are filled in, and the centroid of this region is the centroid of the obscuration. This first centroid calculation can be used as the measurement, or it can be used to define a 32x32 pixel region-of-interest centered on the PSF. Previously, a binary region within this ROI of pixels above a threshold was found and the centroid of the binary region was taken as the PSF location. Now, a gray scale centroid calculation within the ROI is performed to estimate the PSF location.

2. EXPERIMENT

2.1 Purpose

The purpose of the experiment is to assess the stability of the W2-AM centroid measurement. The goal is a centroid measurement with a standard deviation of 50 nrad, and preferably less, to demonstrate the possibility of calibration to that level.

2.2 Initial setup

The first experiment was to assess the W2-AM in essentially the same environment as used on previously reported results. The W2-AM, as shown in the figure below, was mounted on a stand, which in turn was mounted on a small optical breadboard. The breadboard was placed on a cart with pneumatic tires in an office. The return flat was attached directly to the W2-AM.

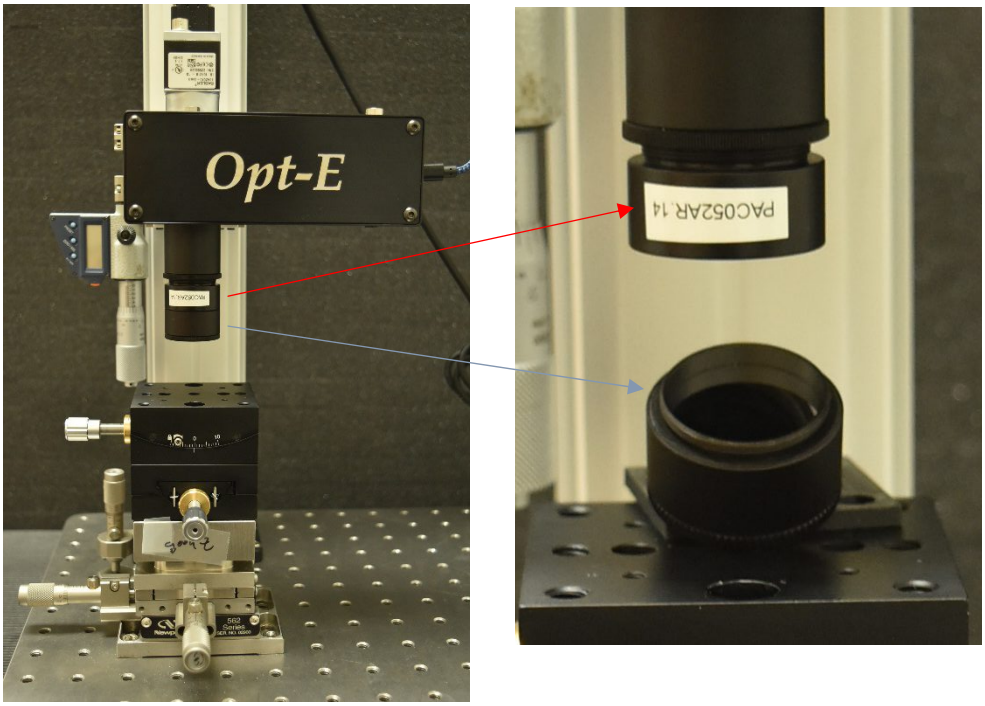

Figure 5. Initial setup: W2-AM mounted to column on a small breadboard resting on a cart with pneumatic tires. The mirror was attached directly to the W2-AM. The mirror is shown separated from the W2-AM in the right image.

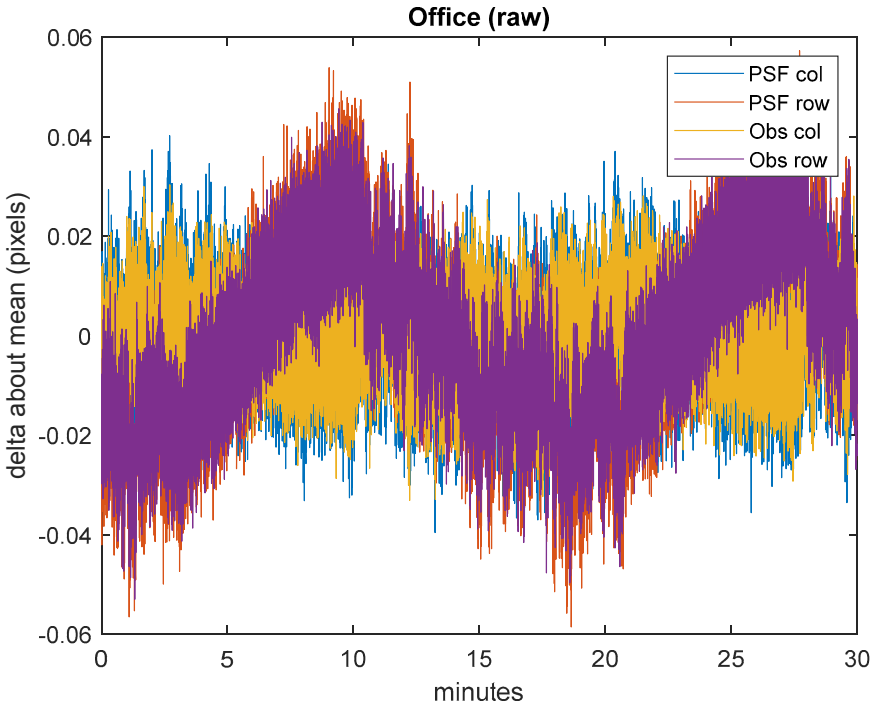

Figure 6 Centroid delta from the mean for the PSF and obscuration taken at 30 Hz for 30 minutes in pixels.

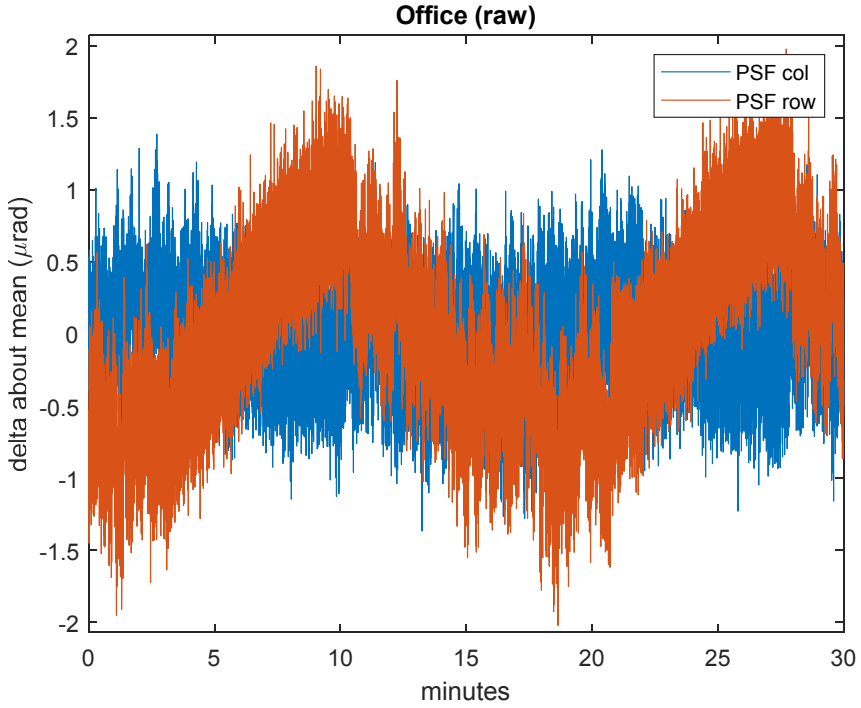

Figure 7. Centroid delta from the mean for the PSF only at 30 Hz for 30 minutes in μrad.

Figure 6 is a plot of centroid position, rows and columns, for both the PSF and obscuration in pixels from the mean position. Unlike previous results where the PSF had approximately ten times more noise than the obscuration, the PSF and obscuration data is very similar to each other. Figure 7 therefore includes only the PSF data since it is preferred for the application since it uses a smaller field-of-view than the obscuration. The plot has also been scaled to µrad, at the same height on the page as the preceding figure. The row centroid shows a very clear cyclic behavior due to air conditioning turning on and off. Though the temperature signal is distinct and very predictable, it is also fairly small scale at about ±1 µrad peak-to-valley in the smoothed data shown in Figure 8 below.

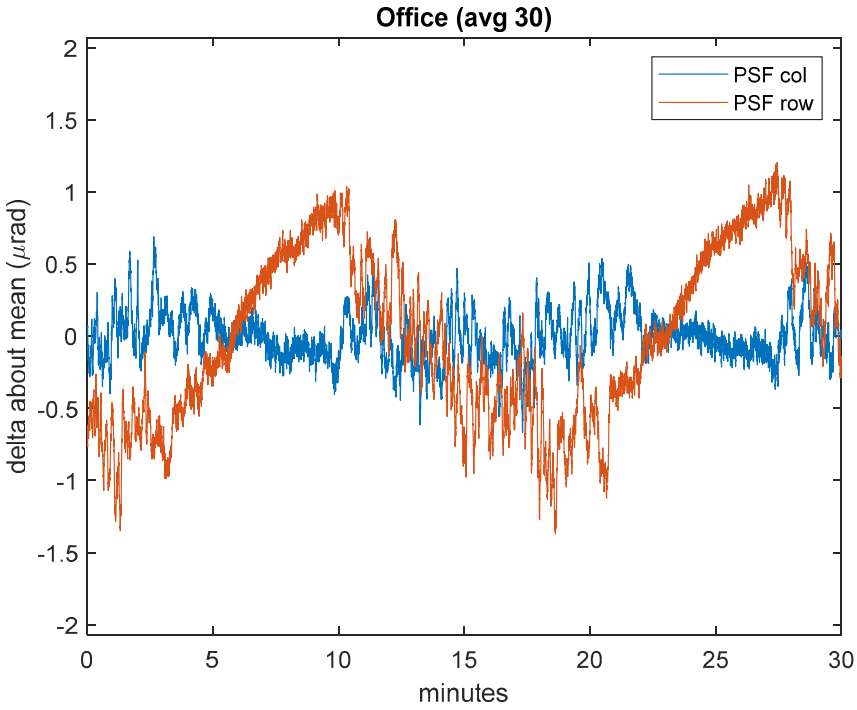

Figure 8. Data from Figure 7 was filtered with a running average of 30 samples.

The variation in the column coordinate in Figures 6-8 is reflected in its standard deviation being larger than the row data in the Table 1. However, the PSF statistics based on a gray scale centroid are now about as good as the standard deviation of the obscuration. Furthermore, a 30-sample running average (1 second) reduces the standard deviation down to 0.17 µrad, or 170 nanorad, in an office. The approach is promising, but a better environment is needed.

Table 1 Standard deviation of centroids from initial setup in office.

First setup	Standard deviation	
	Row	Column
PSF, raw (pixels)	0.0091	0.0183
Obs, raw (pixels)	0.0079	0.0166
PSF, raw (µrad)	0.31	0.63
Obs, raw (µrad)	0.27	0.57
PSF, avg (µrad)	0.17	0.58

2.3 Improved setup

The first change was to move to a cleanroom with at worst ±1°F temperature control and place the W2-AM on a 12'x4'x1' vibration isolation table. Additionally, the W2-AM was clamped to a table, then set on posts, and various configurations of foam insulation was place around the W2-AM.

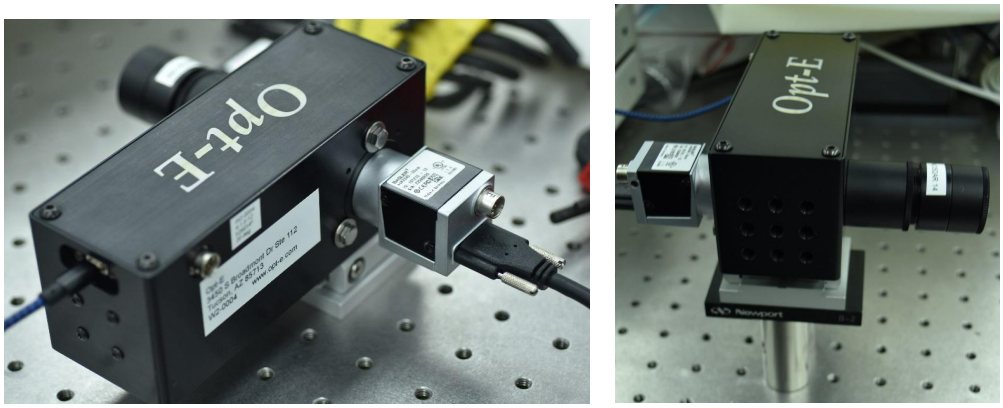

Figure 9. A couple of setups in the clean room on the large optical table. Various configurations of foam insulation are not shown.

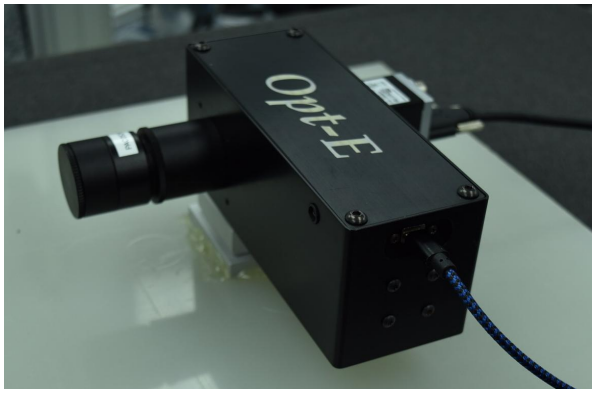

Figure 10. Ultimately, the W2-AM was mounted to a bracket attached to a 12"x12"x1/2" HDPE plate.

Figure 11. The W2-AM was then placed inside a stack of foam with 8" (200 mm) or more foam in each direction.

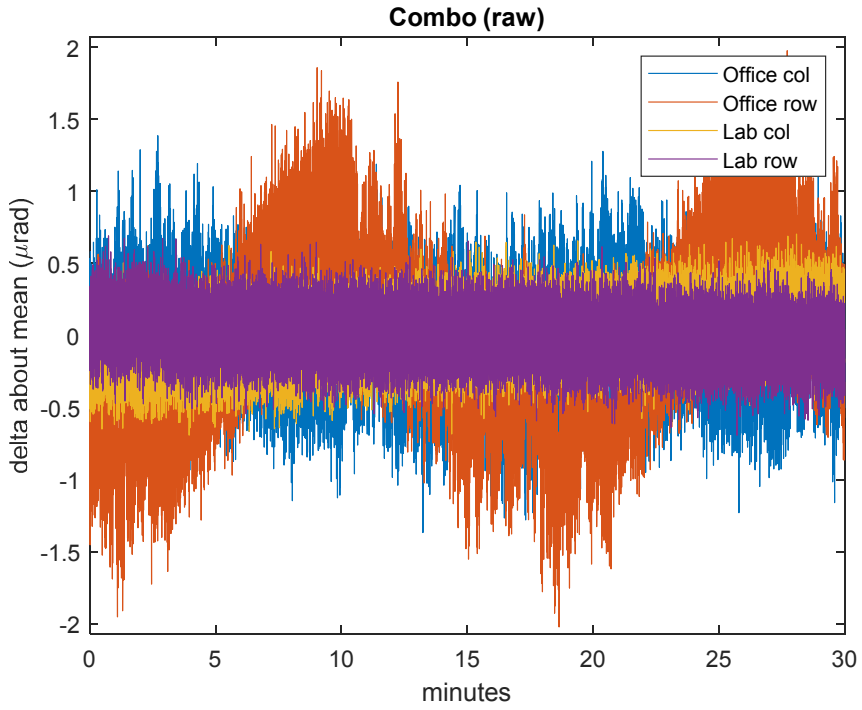

Figure 12. Original PSF centroid office data with lab data.

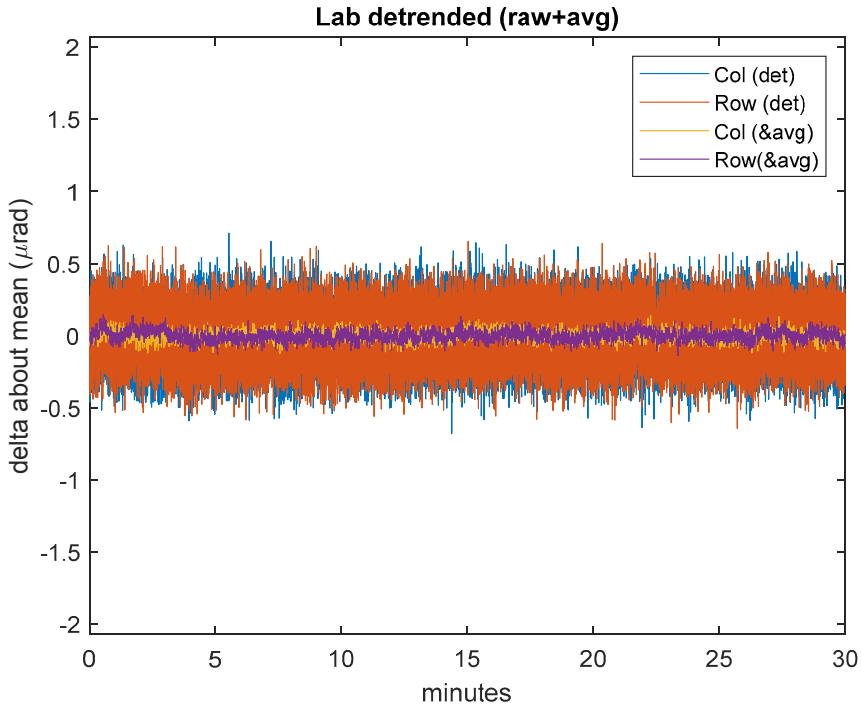

Figure 13. Lab data that has been detrended and averaged data plotted over it.

Table 2 Standard deviation of centroids from final setup in lab.

Final setup PSF only (μrad)	Standard deviation	
	Row	Column
Raw	0.18	0.16
Detrend	0.16	0.16
Detrend & average	0.034	0.035
RSS	**0.048 < 0.050**	

Table 2 summarizes the results of the final setup. The raw data in the lab has a standard deviation about the same as the filtered data from the office. There is still a small trend line, which when removed, results in the row and column standard deviations being equal at 0.16 μrad (160 nrad). A running average of 30 samples results in standard deviations of 0.034 and 0.035 μrad. Combining the standard deviation of the detrended and averaged data results (root-sum-square) results in an estimate of 48 nrad. The results are promising, but there is one consideration that has not been fully addressed.

2.4 Sample area

The results presented above are for a sample area approximately 15 mm in diameter. However, for the application of interest, a sample area between about 2 mm – 5 mm diameter is required. The sample area was reduced by placing an aperture made as shown in Figure 14 below. Apertures of 6.7 mm and 3.7 mm diameters were made. Although in practice apertures are mounted near the optic under test, they are not normally placed in contact with the mirror. For this experiment, the aperture was placed in contact with the mirror.

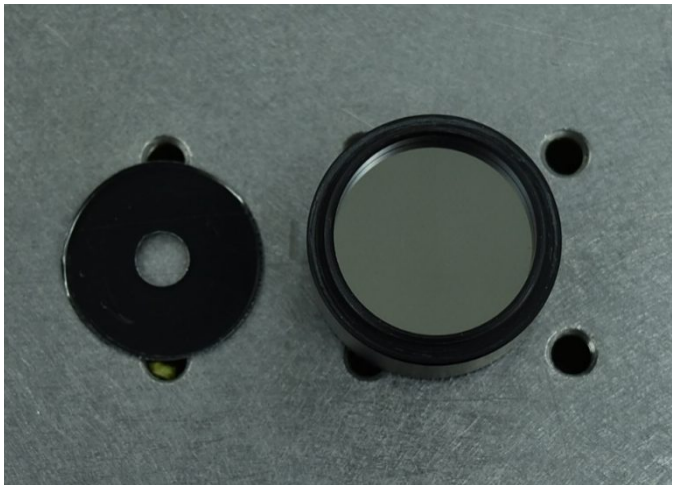

Figure 14. A 6.7 mm diameter aperture in Acktar black material shown next to the 1 in diameter mirror.

In Table 3 below, the standard deviation for centroids with an aperture in contact with the mirror are presented. This experiment had drift in the column. However, the average data for the two aperture sizes is more consistent with the values in three of the four cases being between 0.16 μrad and 0.18 μrad. Even ignoring the outlier, there are two issues: the averaged data here is only about as good as the raw data without the aperture, and the behavior is not significantly affected by aperture size, but only by the mere presence of an aperture at all.

Table 3 Standard deviation of centroids from final setup in lab with aperture in contact with mirror.

Final setup PSF only (μrad)	Standard deviation	
	Row	Column
3.7 mm	0.80	0.92
3.7 mm, average	0.16	0.51
6.7 mm	0.84	0.84
6.7 mm, average	0.16	0.18

The W2-AM projects an aperture out in front of the collimating lens, at about the position of the mirror in these experiments. Instead of placing an aperture on the mirror, the internal aperture size was changed so that an approximately 4.5 mm diameter aperture was projected onto the mirror. The results are shown in Table 4 below. There is drift in the column data; however, the averaged row data has a standard deviation of 98 nrad, which is about 3x the 34 nrad seen in the averaged 15 mm aperture data, for an aperture about 1/3 the diameter. This is a plausible result. However, the desired aperture has a diameter about 2x smaller still. The W2-AM light source was adjusted to provide sufficiently light to use the full dynamic range of the camera without saturation.

Table 4 Standard deviation of centroids from final setup in lab with aperture projects onto mirror.

Final setup PSF only (μrad)	Standard deviation	
	Row	Column
4.5 mm	0.51	0.33
4.5 mm, average	0.098	0.27

3. CONCLUSION

The W2-AM performance has been significantly improved by using a gray scale centroid calculation compared to previous results. The combination of a very good environment, detrending of data and a running average resulted in a centroid standard deviation of about 34 nrad in two orthogonal directions, that when RSS'd together is about 48 nrad. This suggests that with some refinement of the instrument and good environmental controls the W2-AM can obtain this performance in practice.

The W2-AM has benefits in mass and design flexibility that could be beneficial for profiling x-ray optics. However, the small measurement aperture appears to limit the performance of the W2-AM for use in x-ray optics profilometer. The W2-AM is adaptable with the ability to use different cameras, alternative reticle patterns, different projected aperture locations, and perhaps most significantly, with an architecture that makes customized image processing software possible. Additionally, alternative materials, could easily be used for the housing. Even so, improving the performance to the desired level would be challenging, and should consider in great deal, the implications of photon statistics on the measurement approach.

REFERENCES

[1] Takacs, P. Z., Qian, S., and Colbert, J., "Design Of A Long Trace Surface Profiler," Proc. SPIE 0749, Metrology: Figure and Finish, (20 April 1987).

[2] Qian, S., Geckeler, R. D., Just, A., Idir, M., Wu, X., "Approaching sub-50 nanoradian measurements by reducing the saw-tooth deviation of the autocollimator in the Nano-Optic-Measuring Machine," Nuclear Instruments and Methods in Physics Research A 785 (2015) 206-212.

[3] Qian, S., and Idir, M., "Innovative nano-accuracy surface profiler for sub-50 nrad rms mirror test," Proc. SPIE 9687, 8th International Symposium on Advanced Optical Manufacturing and Testing Technologies: Subnanometer Accuracy Measurement for Synchrotron Optics and X-Ray Optics, 96870D (25 October 2016).

[4] Kuhn, W. P., "Design and performance of a new compact adaptable autostigmatic alignment tool," Proc. SPIE 9951, Optical System Alignment, Tolerancing, and Verification X, 995109 (27 September 2016).

[5] Kuhn, W. P., "Measurement of low-order aberrations with an autostigmatic microscope", Proc. SPIE 10377, Optical System Alignment, Tolerancing, and Verification XI, 103770C (22 August 2017).